Chapter 3

Instrumentations and Experimental Techniques

In this chapter, the sample preparing procedures and the sample analysis are briefly summarized. First, the deposition setup including of magnetron sputtering and e-beam evaporation systems using to prepare all magnetic film is described in section 3-1. Then, the metal-metal epitaxy on silicon method used for studying the Os growth is described in section 3-2. The thermal annealing setup and analysis techniques are mentioned in section 3-3 and section 3-4, respectively.

3-1 Deposition setup

In this dissertation, all CoFe/OsMn, CoFe/IrMn and epitaxial Os films were prepared by standard magnetron sputtering system. This system, as shown in Fig. 3-1, has six sputtering sources and six different materials can be deposited in a round without breaking the vacuum. The pumping system contains a mechanic pump and a turbo pump. The best pressure in this system can down to 5×10^{-9} Torr. The film thickness was monitored by quartz microbalance, which was calibrated by atomic force microscope (AFM). The normal deposition process is tuning on the plasma at about 10 ~ 20 mTorr by filling Argon (Ar) gas and, then, tuning the pressure to roughly 3~5 mTorr during deposition. Some parameters are summarized in the Table 3.1.

All PSV films studied in this dissertation were deposited with a dual e-beam evaporation system, as shown in Fig 3-2. In addition, as mentioned in chapter 2, Os films showed poor adhesion to chemically cleaned Si substrate. Thus, the selected buffer layer materials were

also prepared by this e-beam evaporation system and then, the substrate was transferred to the magnetron sputtering system to grow the epitaxial Os film. This system consists of 12 crucibles (6 crucibles per gun) and the pumping system contains a machine pump and a Cryo pump. The best pressure of this system can be down to 5×10^{-8} Torr, while lower than 3×10^{-7} Torr during each sample deposition with the deposition rate keeping around 0.1nm/sec. Like magnetron sputtering system, the film thickness was also monitored by quartz microbalance, which was also calibrated by AFM. Some parameters are summarized in the Table 3.2.

Table 3.1 Deposition conditions of the magnetron sputtering system

	Power	I (A)	P (torr)	Rate (Å/sec)
Cu	20W, 400V	0.06	$3.1*10^{-3}$	2.0
Os	20W, 380V	0.06	$2.5*10^{-3}$	0.9
IrMn	10W, 310V	0.04	$4.2*10^{-3}$	1.0
CoFe	40W, 287V	0.17	$6.0*10^{-3}$	1.0
Pd	10W, 263V	0.04	$1.9*10^{-2}$	5.0

Table 3.2 Deposition conditions of the E-gun evaporation system

	P_i (torr)	I (A)	P (torr)	Rate (Å/sec)
$Ni_{80}Fe_{20}$	$1.6*10^{-7}$	0.41	$1.7*10^{-7}$	1.0
Co	$1.6*10^{-7}$	0.4	$1.7*10^{-7}$	1.0
Cu	$1.7*10^{-7}$	0.38	$1.8*10^{-7}$	1.0
Ta	$1.6*10^{-7}$	1.4	$4.4*10^{-7}$	1.0
Ti	$1.9*10^{-7}$	0.38	$1.2*10^{-7}$	1.0
Au	$1.9*10^{-7}$	0.48	$4.3*10^{-7}$	1.0
Ag	$1.6*10^{-7}$	1.26	$2.9*10^{-7}$	1.0
SiO_2	$3.5*10^{-7}$	1.08	$1.0*10^{-6}$	1.2
Pd	$1.9*10^{-7}$	1.27	$2.2*10^{-7}$	1.0

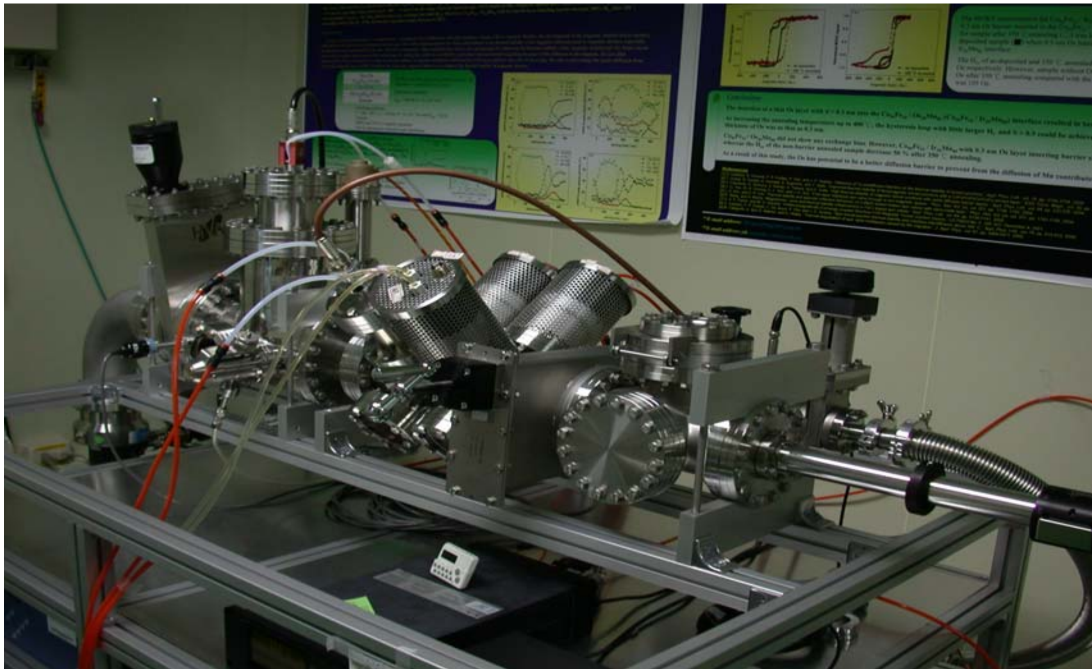

Fig. 3-1 Image of the magnetron sputtering setup. This system has six sputtering guns with different materials, and the base pressure is below 5×10^{-9} Torr.

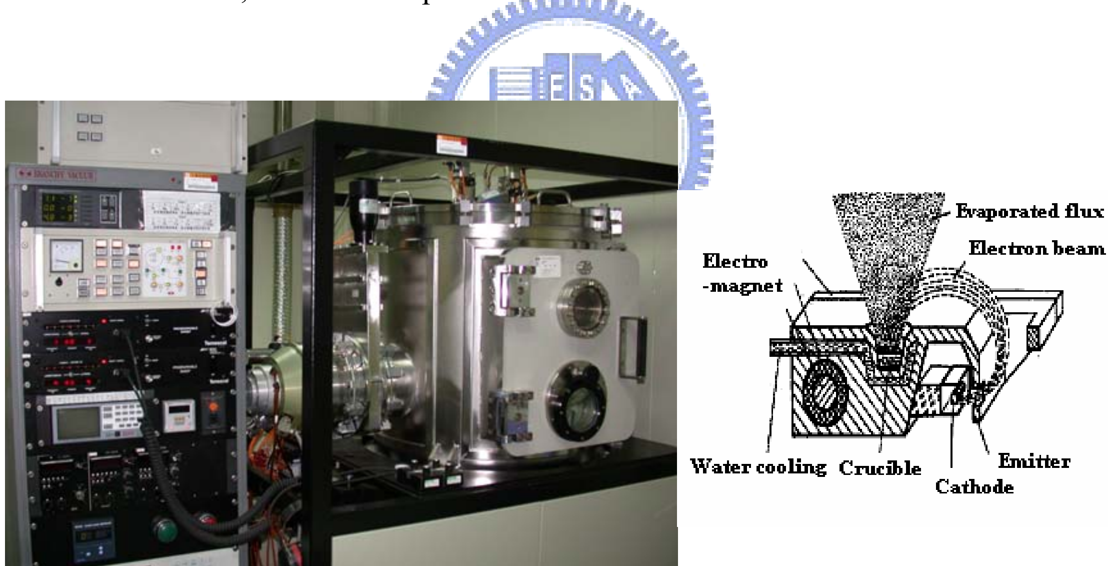

Fig. 3-2 Image of the E-gun evaporation system. This setup includes 12 crucibles which can hold 12 different materials, and the best pressure is 5×10^{-8} Torr.

3-2 Metal-Metal Epitaxy on Silicon Method (MMES)

In 1990, Chang reported that using electron beam evaporation without intentional heating of the substrates, (001) and (111) Cu epitaxial films can be grown on hydrogen terminated (001) and (111) Si, respectively [100]. Furthermore, it is of interest to use the Cu film as the seed layer for additional epitaxial growth of metal films. The growth of metal films with the (001) orientation for both fcc and bcc metal, starting with the (001) Cu films epitaxially grown on (001) Si as seed layer, was reported. The fcc metal grown by this technique include Ni, Co [101], Rh, Ir [102], Pd, Au, Ag, Pt [103], and Al [104], and the bcc metals include Fe, Cr, V, Mo, W [105]. This technique was called metal-metal epitaxy on silicon (MMES). Indeed, the epitaxial growth of Cu on Si was found to depend on the cleanliness of the silicon substrate surface. For example, (111) textured Cu films were found to grow on atomically clean (2×1) Si (001) reconstructed surface and (001) epitaxial films grown on hydrogen terminated (1×1) Si (001) reconstructed surface [106]. Furthermore, it has been shown that such hydrogen terminated surfaces are known to be inert for several minutes in air and for several hours in high vacuum at room temperature [107]. This surface passivation is believed to be due to hydrogen termination of the dangling Si bounds, which renders the chemically stable surface [106]. During the growth of Cu on Si (001) at room temperature, it was found that interdiffusion between Cu and Si occurred within a region about 100 Å, resulting in the formation of Cu3Si silicide, which adjusted the lattice mismatch between Cu and Si [108]. The epitaxial relationship between Cu and Si (001) was found to be Si (001)//Cu (001) and Si [110]// Cu [010], as schematically illustrated in Fig. 3-3. Fig. 3-4 is the XRD diffraction pattern of Cu grown on H-Si (100), and the clear Cu (002) peak can be observed even though the Cu was only 30 nm.

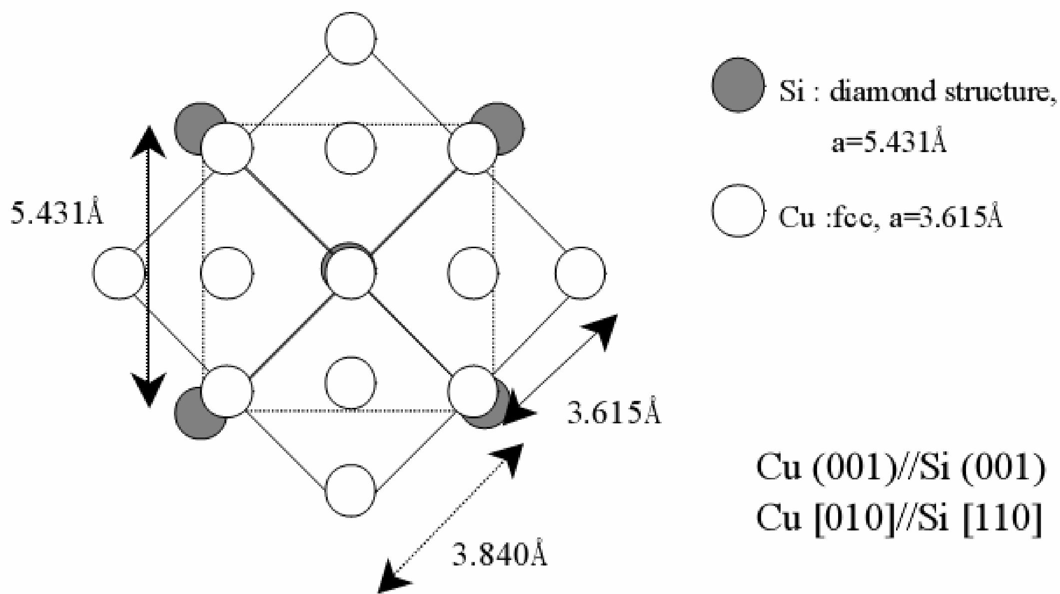

Fig. 3-3 Schematic illustration of the epitaxial relationships between Cu and Si (001). The epitaxial relationships are: Cu (001) // Si (001) and Cu [010] // Si [110].

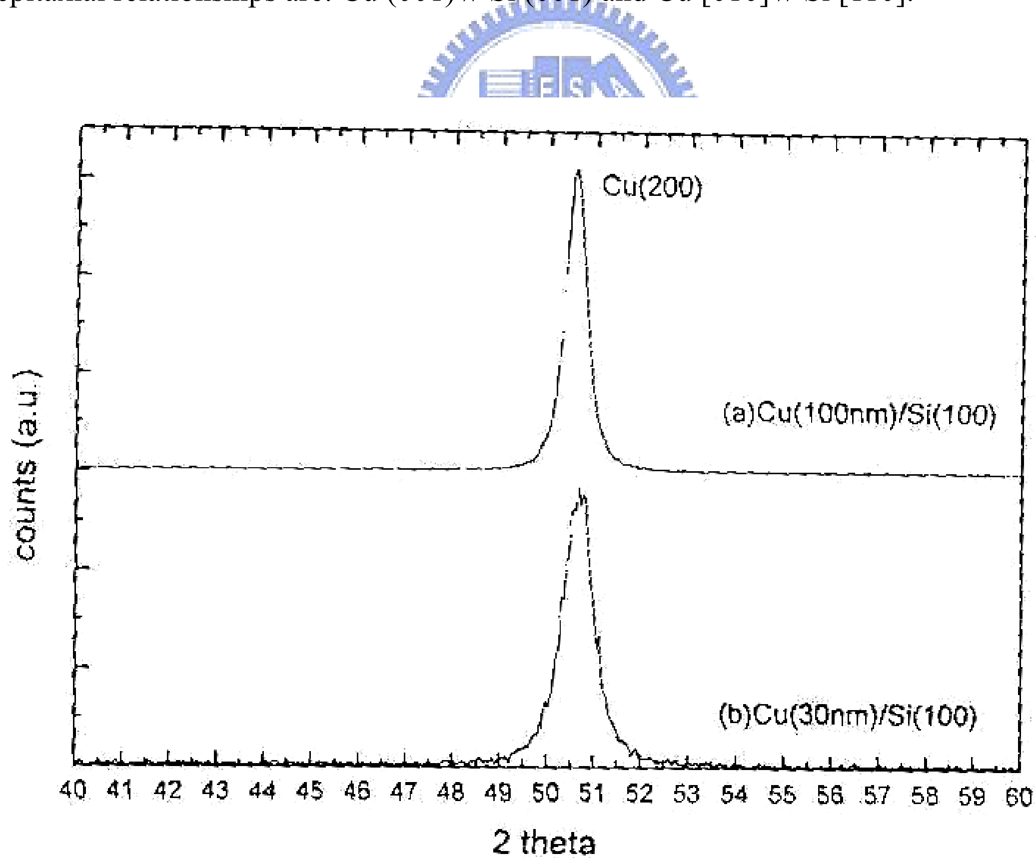

Fig. 3-4 The XRD pattern of Cu grown on H-Si (100) by MMES method. The Cu (002) peak can be observed clearly even the Cu file was only 30 nm. (Data are from [142])

3-3 Thermal annealing setup

In general, Mn-based antiferromagetic films are subjected to a post filed annealing treatment to enhance the exchange field due to the (111) crystalline structure can be improved. In this dissertation, the field annealing, as shown in Fig 3-5, was used to examine the thermal stability of the magnetic FM/AFM films. The annealing system contains an electromagnet and a vacuum anneal chamber. Samples were loaded into the camber and were heated to the needed temperature after the vacuum lower than 1×10^{-2} Torr. The samples were be kept a period under an applied filed when reach the annealing temperature. Then, the samples were natural cooling down to room temperature. The range of the annealing temperature and applied field was 150 ~ 450°C and 1 ~ 4 kOe, respectively. There are some parameters of the annealing setup summarized in Table 3.3.

Table 3.3 Parameters of the field annealing system

I (A)	H (Oe)	V (V)
3.106	500	6.68
6.3	1000	13.35
9.4	1500	19.92
12.6	2000	26.7
16	2500	33.92
19	3000	40.36
22.1	3500	47
25.7	4000	55

Fig. 3-5 Image of the field annealing setup. This system has an electromagnet and a vacuum anneal chamber, and the working pressure is 1×10^{-3} Torr.

3-4 Analysis techniques

In this study, magnetic properties were measured by vibration sample magnetometer (VSM) and magneto-optical Kerr effect (MOKE). Fig. 3-6 illustrates the MOKE setup. The principle of MOKE is that the rotation of the linear polarized laser beam during reflection from a magnetized specimen. The amount of rotation depends on the direction and magnitude of the magnetization relative to the plane of incidence of the laser beam. As shown in Fig. 3-6, the linear polarized He-Ne laser light by polarizer is introduced into the sample located at the center of the electromagnet. If the sample is magnetized by the field, the induced magnetization of the sample would change the dielectric tensor of the sample form diagonal-only form to the non-diagonal form. This complex tensor would change the linear polarized light, and the reflected light from the sample thus has the elliptical polarization. One can tune the magnetization of the sample by controlling the applied field to change the ellipticity and tilted angle of the elliptical reflected light from the sample. In our setup, the reflected light is guided into another linear polarizer, and then into a photo-diode. Theoretically, the photo-diode voltage by the reflected light, which called Kerr intensity, is proportional to the magnetization of the sample. Therefore, the hysteresis loop of the sample can be measured.

The film structure was characterized by X-ray diffraction (XRD, Siemens D-5000) with the wavelength of Cu K_α and transmission electron microscope (TEM). For better S/N ratio of the XRD signal, the slower scan velocity of 2.5 min/deg was used. To avoid the monitoring the signals coming from Si substrates, the measurement range of 2θ was fixed from 35° ~ 55°, and the main diffraction peaks of Si (400) ($2\theta = 69.132°$) and Si (111) ($2\theta = 28.443°$) were not detected in this range.

Auger Electron Spectroscopy (AES, Thermo VG Microlab-350) depth profile was used to detect composition distribution along the surface normal. Typically AES has a resolution of 2 nm depth at normal depth analytical condition, low ion energy etching (1 keV) and low electron take-off angle detection (30°) were necessary for the sub-nm depth resolution in ultra-thin film depth analysis. Peaks overlap problem was happened at Co, Fe, and Mn main peaks (as shown in Fig. 3-7), and the minor peak, LM2 or LM3, was chosen in this study.

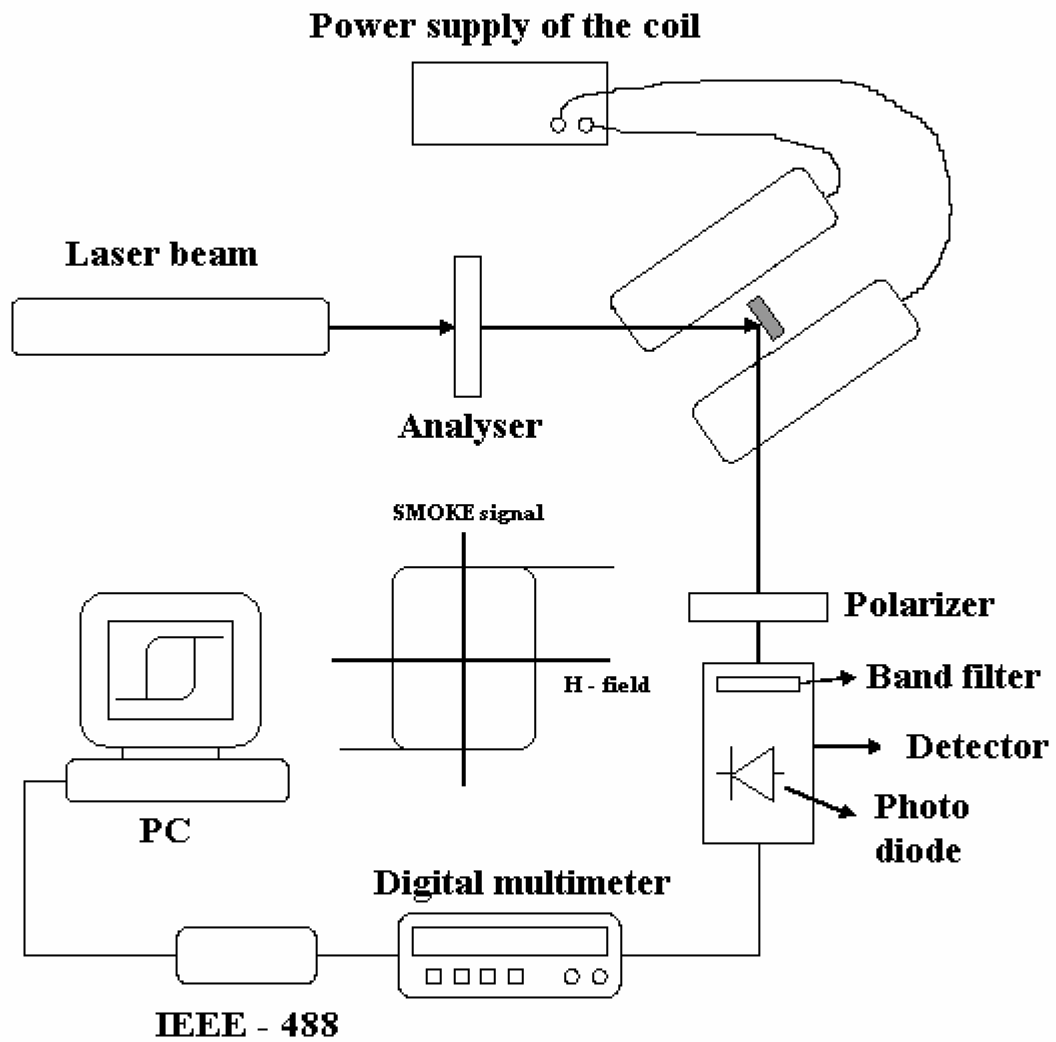

Fig. 3-6 Schematic illustration of the MOKE setup.

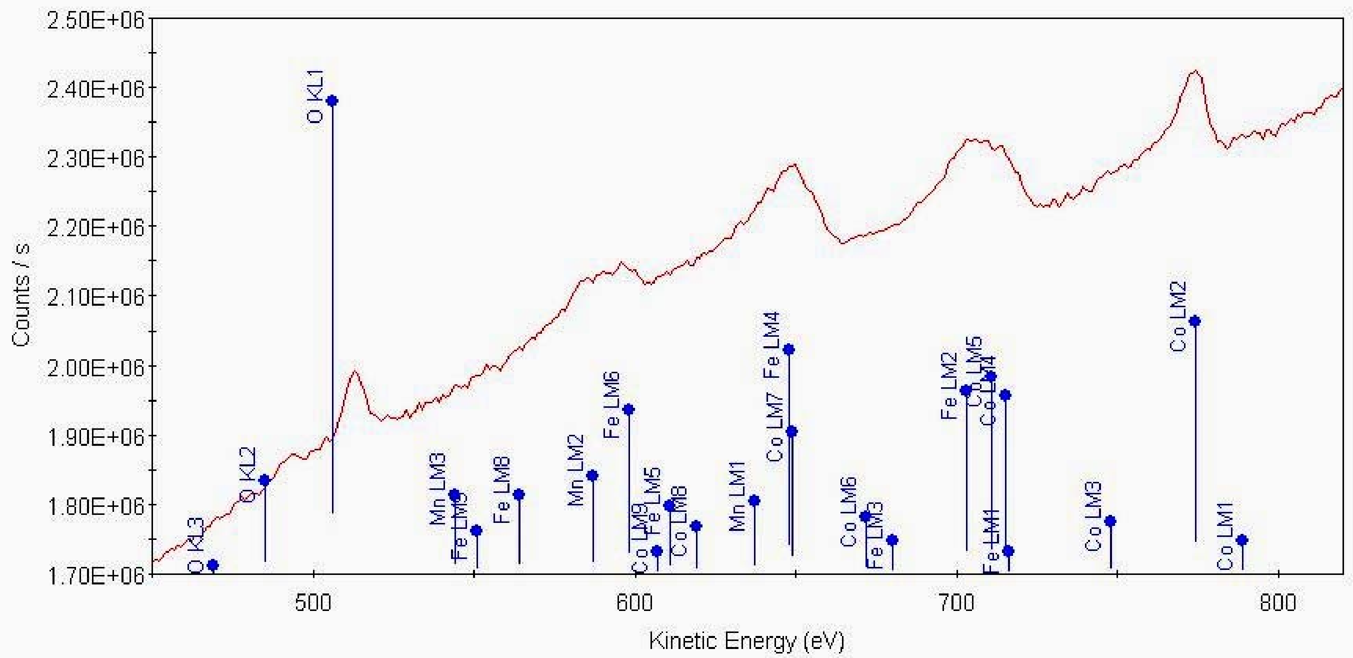

Fig. 3-7 The Auger electron spectrum on the surface in the CoFe layer. The main peaks of Co, Mn, and Fe were overlapped in this energy range.